applied sciences

MDPI

Article

A Three-Objective Optimization Model for Sustainable Power System Design: Balancing Costs, Emissions and Social Opposition

Cristian Cafarella *, Michele Ronchi, Francesco Gabriele Galizia, Marco Bortolini and Mauro Gamberi

Department of Industrial Engineering, University of Bologna, Viale del Risorgimento 2, 40136 Bologna, Italy; michele.ronchi8@unibo.it (M.R.); francesco.galizia3@unibo.it (F.G.G.); marco.bortolini3@unibo.it (M.B.); mauro.gamberi@unibo.it (M.G.)

* Correspondence: cristian.cafarella2@unibo.it

Abstract

The design of sustainable power systems requires planning tools that jointly account for economic, environmental, and social dimensions. However, multi-objective energy system models typically prioritize economic–environmental trade-offs, while the social dimension is still rarely included as an explicit optimization objective. Furthermore, many formulations adopt a low temporal resolution (e.g., annual time steps) and assume fully flexible power plants, potentially overlooking temporal variability and operational constraints. This paper presents a three-objective optimization model for sustainable power system design that minimizes (i) costs, (ii) greenhouse gas (GHG) emissions, and (iii) social opposition (i.e., the public resistance to certain energy technologies). Temporal variability and operational detail are preserved using weighted representative periods with intra-period time steps and a clustered unit commitment (CUC) formulation. The Pareto frontier is generated using the normalized normal constraint (NNC) method, highlighting the space of efficient economic, environmental, and social solutions. A case study focused on the Italian electricity system exemplifies the model application by providing the cost-optimal, emissions-optimal, and social-optimal solutions, together with trade-off solutions. Among the trade-off solutions, the selected best balance solution achieves a significant reduction in emissions (−20%) compared to the cost-optimal solution, with a limited cost increase (+5%) and a marginal increase in social opposition (+0.7%). Overall, the proposed model enables transparent quantification of multi-dimensional trade-offs to support decision-making in sustainable power system design.

Keywords: generation expansion planning; multi-objective optimization; power system modeling; sustainable development; renewable energy sources

Academic Editor: Paulo Santos

Received: 18 February 2026
Revised: 5 March 2026
Accepted: 17 March 2026
Published: 18 March 2026

1. Introduction

The transition toward sustainable energy systems calls for planning tools that can guide investment decisions while balancing multiple dimensions of sustainability [1–3]. In power system design, decision makers increasingly face objectives, often mutually conflicting, that go beyond least-cost planning and include environmental and social concerns [3].

In such a context, the role of energy planners is to communicate the results of energy system modeling and scenario generation to decision makers in a transparent and comprehensive way. In this regard, Prina et al. [4] highlight that multi-objective optimization provides relevant advantages over single-objective optimization. Specifically, single-objective optimization returns one optimal solution per run, whereas multi-objective optimization identifies a set of Pareto-optimal solutions that explicitly represents the trade-offs among competing objectives.

The literature also indicates that model outcomes can be strongly affected by the representation of temporal resolution and operational detail [4–7]. As the penetration of variable renewable energy (VRE) sources increases, together with storage deployment and the need for flexibility, a finer temporal resolution becomes increasingly important to capture variability and operational patterns reliably [4,5]. However, energy system planning models often rely on simplified temporal representations to keep the optimization problem tractable, which may introduce non-negligible approximation errors and bias key results, such as renewable curtailment, storage operations, and the utilization of dispatchable generation [6]. A similar trade-off arises for operational detail. Due to computational restrictions, several energy system planning models adopt simplified operational representations, often omitting unit commitment (UC) decisions and key operational constraints and cost components, such as start-up costs, minimum up/down times, minimum operating point, and ramping limits and costs [4]. The literature warns that neglecting these constraints can distort technology valuation and lead to inaccurate estimates of operational and total system costs, particularly in high-renewable systems [7].

Overall, these findings motivate modeling strategies that balance computational tractability and solution accuracy by combining reduced temporal representations with sufficient intra-period resolution [8] and an adequate level of operational detail [9].

1.1. Literature Review

In recent years, multi-objective energy system models have received increasing attention, driven by the recognition that the traditional least-cost planning paradigm can be insufficient to capture the complexity of energy transition challenges [1–3]. In this context, this section provides a targeted overview of methodological approaches, objectives, and key modeling choices to position this paper and highlight research gaps.

Table 1 provides an overview of representative contributions on multi-objective energy system planning models. The studies are classified according to: (i) objective categories covered (economic, environmental, and social), (ii) multi-objective setup (number of objectives and solution method), (iii) temporal resolution, and (iv) operational detail.

The literature review shows a clear prevalence of bi-objective formulations centered on the economic–environmental trade-off. Most studies model the economic dimension through the minimization of total system costs, while the environmental dimension is commonly represented through the minimization of greenhouse gas (GHG) emissions, yielding a cost–emissions bi-objective setting [10–19].

Alongside the cost–emissions formulation, other studies extend the objective space by considering alternative environmental and economic objectives. For instance, Cafarella et al. [20] replace emissions with land use in a bi-objective cost–land formulation. Other contributions move to three-objective formulations. Peng et al. [21] combine costs, emissions, and a risk measure based on the conditional value-at-risk of total cost. Prebeg et al. [22] propose a formulation that minimizes the net present value (NPV) and a normalized NPV (defined as NPV divided by the total energy produced to cover demand), while maximizing the renewable energy share. Parkinson et al. [23] extend the environmental dimension by including the minimization of groundwater extraction, alongside costs and emissions.

The social dimension is still rarely included as an explicit optimization objective in multi-objective energy system models. Shidhani et al. [24] formulate a broader set of sustainability criteria by considering costs and emissions together with land use and social opposition. However, instead of optimizing these criteria simultaneously, they explore trade-offs through a sequence of pairwise bi-objective optimization, generating Pareto-front candidates for each objective pair. Trotter et al. [25] combine system costs with two sub-national electrification-inequality indicators, capturing urban–rural disparities and inter-regional disparities. Atabaki et al. [26] explicitly include the three sustainability dimensions in a three-objective formulation by combining costs, emissions, and job creation.

Table 1. Classification of literature contributions on multi-objective energy system modeling (✓ = objective category covered, BO = bi-objective, TO = three-objective, WS = weighted sum, EC = ε-constraint, AHP = analytic hierarchy process, MOEA = multi-objective evolutionary algorithms, NNC = normalized normal constraint, RPM = reference point method, RP = representative periods, FF = fully flexible, SU = start-up, MUT = minimum up time, MDT = minimum down time, MOP = minimum operating point, RAMP = ramping).

Reference	Economic	Environmental	Social	Multi-Objective Setup	Temporal Resolution	Operational Detail
Purwanto et al. [10]	✓	✓		BO (WS)	years	FF
Gbadamosi et al. [11]	✓	✓		BO (WS)	years	FF
Pratama et al. [12]	✓	✓		BO (WS)	years	FF
Groissböck et al. [13]	✓	✓		BO (WS)	RP (night/day)	FF
Finke et al. [14]	✓	✓		BO (EC)	RP (hours)	SU, RAMP
Louis et al. [15]	✓	✓		BO (EC)	RP (hours)	MUT, MDT, MOP, RAMP
Prina et al. [16,17]	✓	✓		BO (MOEA)	hours	FF
Viesi et al. [18]	✓	✓		BO (MOEA)	hours	FF
Prina et al. [19]	✓	✓		BO (MOEA)	hours	SU, RAMP
Cafarella et al. [20]	✓	✓		BO (NNC)	RP (hours)	SU, MUT, MDT, MOP, RAMP
Peng et al. [21]	✓	✓		TO (MOEA)	years	FF
Prebeg et al. [22]	✓	✓		TO (MOEA)	years	FF
Parkinson et al. [23]	✓	✓		TO (RPM)	months	FF
Shidhani et al. [24]	✓	✓	✓	BO (MOEA)	years	FF
Trotter et al. [25]	✓		✓	TO (EC)	years	FF
Atabaki et al. [26]	✓	✓	✓	TO (AHP)	years	FF
This paper	✓	✓	✓	TO (NNC)	RP (hours)	SU, MUT, MDT, MOP, RAMP

Multi-objective optimization methods can significantly affect both the efficiency and the optimization results of energy system models. Based on when decision makers articulate preferences, multi-objective methods are commonly classified into prior (preferences specified before the search), posterior (preferences applied after generating a set of efficient solutions), and interactive approaches (preferences updated during the search). In the reviewed studies, prior methods include the weighted sum (WS) method [10–13], the ε-constraint (EC) method [14,15,25], and the analytic hierarchy process (AHP) [26]. Posterior methods include multi-objective evolutionary algorithms (MOEA) [16–19,21,22,24] and the normalized normal constraint (NNC) method [20]. An interactive approach is adopted by Parkinson et al. [23], using the reference point method (RPM).

A further point of differentiation concerns the adopted temporal resolution. Several models adopt a lower temporal resolution using years [10–12,21,22,24–26] or months [23] as time steps, which supports long-horizon tractability but tends to smooth short-term variability and operational patterns that become critical in high-renewable systems. Conversely, some models adopt a full hourly representation [16–19], improving operational realism at the cost of a substantially higher computational burden. An intermediate strategy relies on representative periods, which compress the annual time domain while retaining finer intra-period dynamics, either through hourly resolution within representative days/weeks [14,15,20] or through simplified representative slices (e.g., night/day) [13]. The literature explicitly frames the use of representative periods as a trade-off between computational tractability and the ability to represent the variability of renewables, storage and flexibility requirements [8].

Furthermore, the representation of operational detail remains limited in multi-objective energy system models. Many models treat dispatchable power plants as fully flexible [10–13,16–18,21–26], thereby omitting detailed operational constraints (e.g., start-up costs, minimum up/down times, minimum operating point, and ramp-rate restrictions), whereas only a few models adopt a UC formulation and include detailed operational constraints [15,20]. The literature shows that neglecting unit-commitment constraints can bias technology valuation and lead to an underestimation of operational costs, particularly at high renewable penetration [7].

1.2. Research Gap and Contribution

The literature review highlights that multi-objective energy system models are largely dominated by formulations centered on the economic–environmental trade-off, while the social dimension remains less represented as an optimization objective. Moreover, many models rely on coarse temporal representations based on yearly or monthly time steps, which support tractability but tend to smooth short-term variability and operational patterns that become critical in high-renewable systems. Due to computational restrictions, operational detail is also often simplified in multi-objective energy system models, with dispatchable power plants frequently treated as fully flexible. This implies omitting UC decisions and key operating constraints and cost components, which can bias technology valuation and lead to an underestimation of operational costs, especially in systems with high renewable penetration.

Overall, to the best of our knowledge, no existing model simultaneously addresses the economic, environmental, and social dimensions within a three-objective formulation while combining a high level of temporal and operational detail.

To address these gaps, this paper proposes a three-objective optimization model for sustainable power system design with the following main contributions:

- Three-objective sustainability formulation that simultaneously minimizes total system costs, GHG emissions, and social opposition (defined as public resistance to certain energy technologies), with the Pareto frontier explored via the NNC method.
- The target year is represented through weighted representative periods with intra-period time steps, providing a tractable yet temporally detailed representation of demand and VRE variability, and dispatchable technologies are modeled through a clustered unit commitment (CUC) approach that retains key commitment decisions and operating constraints/cost components while limiting computational burden.
- A case study focused on the Italian electricity system in a brownfield setting for a 2040 planning horizon, demonstrates how the proposed approach can quantify and communicate multidimensional trade-offs among economic, environmental, and social objectives.

Although the individual components of the proposed approach have been studied in the literature, the contribution of this work lies in integrating them into a single optimization framework. In this integrated setting, weighted representative periods and the CUC formulation jointly provide an operationally consistent representation of variability and commitment-driven constraints while maintaining computational tractability. This allows the trade-offs among total system costs, GHG emissions, and social opposition to be assessed on a consistent operational basis, rather than relying on simplified operational assumptions. Finally, the NNC method is adopted to systematically construct a well-distributed representation of the Pareto frontier in the three-objective space, supporting a transparent characterization of efficient solutions and their trade-offs.

2. Materials and Methods

This section presents the proposed methodology. Section 2.1 introduces the adopted notation, Section 2.2 outlines the problem statement and assumptions, and Section 2.3 details the mathematical formulation of the three-objective optimization model, including the objective functions and constraints.

2.1. Nomenclature

The notation used is reported below, which defines the sets, parameters, and decision variables. Parameters are denoted by uppercase letters, whereas decision variables are denoted by lowercase letters.

2.1.1. Sets

- $k \in K$: energy technologies (generation and storage)
- $p \in P \subseteq K$: generation technologies
- $p \in H \subseteq P$: thermal generation technologies
- $p \in R \subseteq P$: variable renewable generation technologies
- $s \in S \subseteq K$: storage technologies
- $i \in I$: representative periods
- $t \in T$: time steps within each representative period

2.1.2. Parameters

- W_i: repetitions of representative period in one year
- Δ_t: time-step duration
- C_k^{INV}: annualized investment cost
- C_k^{FOM}: fixed operation and maintenance cost
- C_p^{VOM}: variable operation and maintenance cost of generation
- C_s^{VOM}: variable operation and maintenance cost of storage
- C_p^{FU}: fuel cost, $p \in H$
- C_p^{EM}: emission cost, $p \in H$
- C_p^{SU}: start-up cost, $p \in H$
- C_p^{RAMP}: ramping cost, $p \in H$
- EF_p: emission factor, $p \in H$
- SO_p: social opposition
- $DM_{i,t}$: electrical power demand
- CP_k^{EX}: existing installed capacity
- CP_k^{MAX}: maximum new installable capacity
- AF_k: availability factor
- P_p^{MIN}: minimum stable power output per unit, $p \in H$
- P_p^{MAX}: maximum power output per unit, $p \in H$
- SU_p: maximum start-up power per unit, $p \in H$

https://doi.org/10.3390/app16062946

- SD_p: maximum shut-down power per unit, $p \in H$
- RU_p: maximum ramp-up rate, $p \in H$
- RD_p: maximum ramp-down rate, $p \in H$
- MUT_p: minimum up-time in time steps, $p \in H$
- MDT_p: minimum down-time in time steps, $p \in H$
- $CF_{p,i,t}$: time-dependent capacity factor, $p \in R$
- PE_s: power-to-energy ratio
- RT_s: round-trip efficiency

2.1.3. Decision Variables

- c^{inv}: annual invest cost
- c^{om}: annual operation and maintenance cost
- c^{gen}: annual generation cost
- c^{flex}: annual flexibility cost
- cp_k^{in}: installed capacity
- cp_k^{new}: new installed capacity
- cp_k^{av}: available capacity (cp_p^{av} denotes available power capacity for $p \in P$ and cp_s^{av} denotes available energy capacity for $s \in S$)
- $g_{p,i,t}$: electrical power generation
- $f_{s,i,t}^{+}$: charging electrical power
- $f_{s,i,t}^{-}$: discharging electrical power
- $ramp_{p,i,t}$: change in power output (ramp), $p \in H$
- u_p^{av}: number of available units, $p \in H$
- $u_{p,i,t}^{on}$: number of online units, $p \in H$
- $u_{p,i,t}^{su}$: number of starting-up units, $p \in H$
- $u_{p,i,t}^{sd}$: number of shutting-down units, $p \in H$
- $curt_{p,i,t}$: renewable curtailment (unused available output), $p \in R$
- $soc_{s,i,t}^{fr}$: state of charge in the first repetition of representative period
- $soc_{s,i,t}^{lr}$: state of charge in the last repetition of representative period

2.2. Problem Statement and Assumptions

We consider a brownfield power system planning setting, where the existing technology portfolio provides the starting point and can be expanded through new capacity investments. Accordingly, the set of technologies $k \in K$ includes both existing and candidate technologies, comprising $p \in P$ generation (thermal $p \in H$ and variable renewable $p \in R$) and $s \in S$ storage technologies.

Based on three distinct objectives, i.e., minimizing costs, GHG emissions, and social opposition, the proposed model determines: (i) which technologies are deployed, (ii) their optimal expansion size (cp_k^{new}), and (iii) the optimal system operation required to meet demand at each time step, in terms of generation ($g_{p,i,t}$), renewable curtailment ($curt_{p,i,t}$), and storage charging/discharging ($f_{s,i,t}^{+}$, and $f_{s,i,t}^{-}$). Solving the resulting multi-objective problem yields the Pareto frontier, providing a transparent set of efficient trade-off solutions to support decision-making.

The UC constraints of thermal generation technologies $p \in H$ are represented through a CUC formulation, which aggregates similar units into clusters and replaces per-unit binary commitment variables with cluster-level variables tracking the number of online, starting-up, and shutting-down units ($u_{p,i,t}^{on}$, $u_{p,i,t}^{su}$, and $u_{p,i,t}^{sd}$). As discussed in the literature [7,9], for longer-term operational studies and generation expansion planning problems, incorporating a traditional binary unit commitment (BUC) formulation at the individual-unit level is typically computationally infeasible. CUC formulations are therefore adopted to reduce the computational burden associated with BUC formulations by

eliminating a large number of identical or very similar commitment decisions [7,9]. For instance, Meus et al. [9] show that CUC can preserve planning-relevant commitment and dispatch patterns with limited deviations compared to BUC, while providing substantial computational savings.

The number of time steps strongly affects the number of variables and constraints, leading to substantial computational challenges as the problem size increases [27]. To keep the optimization tractable while capturing the variability of electricity demand ($DM_{i,t}$) and renewable generation potential ($CF_{p,i,t}$), the target year is represented by a set of representative periods $i \in I$ (e.g., days), each composed of $t \in T$ time steps (e.g., hours) and weighted by W_i (i.e., the number of times representative period $i \in I$ is repeated within one year).

Figure 1 provides an overview of the considered planning problem, highlighting the connections between the main components and decision variables.

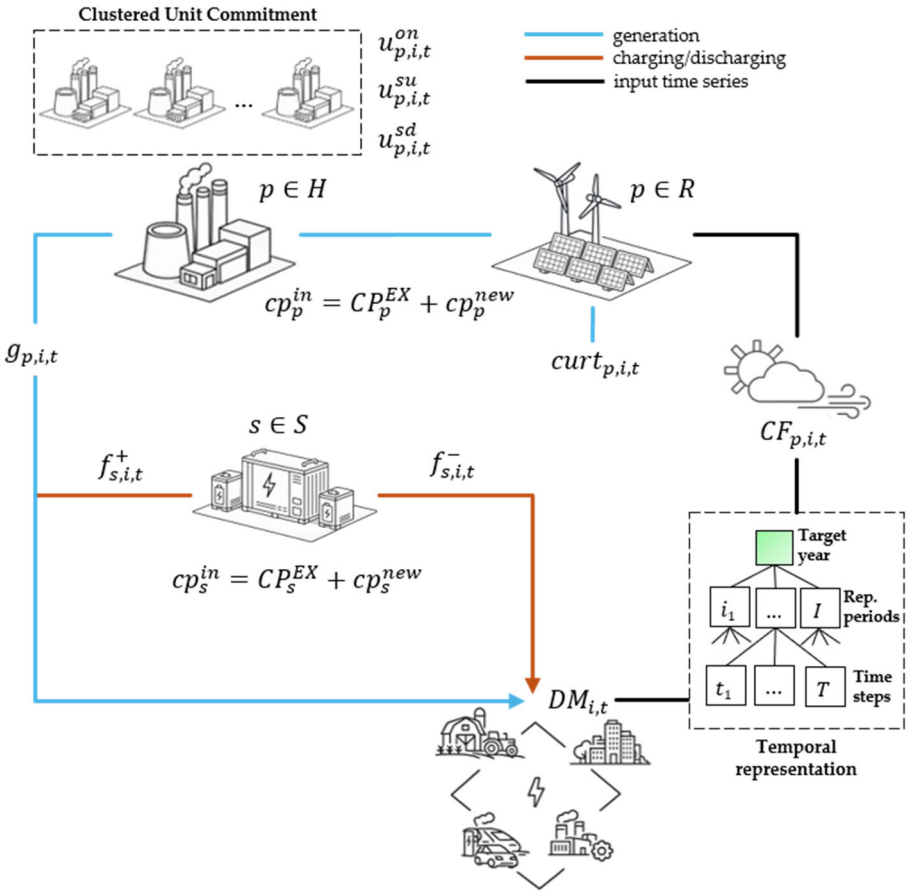

Figure 1. Problem overview. For the notation see the parameters, sets, and decision variables subsections.

2.3. Mathematical Model Formulation

The mathematical formulation of the proposed three-objective optimization model is detailed below. Depending on whether the unit-commitment variables are relaxed as continuous or enforced as integers, the model can be solved either as a linear programming (LP) or a mixed-integer linear programming (MILP), respectively. All other decision variables are continuous and non-negative. All sets, parameters, and decision variables used in the formulation are defined in Section 2.1.

2.3.1. Objective Functions

The cost function, given in Equation (1), minimizes the total annual system cost. This cost is defined as the sum of annualized investment costs, operation and maintenance costs (fixed and variable), generation costs (fuel and emission), flexibility costs (start-up and ramping). These cost components are computed in Equations (2)–(5), respectively.

$$\min \phi_{cost} = c^{inv} + c^{om} + c^{gen} + c^{flex} \tag{1}$$

$$c^{inv} = \sum_{k \in K} \left(C_k^{INV} cp_k^{new} \right) \tag{2}$$

$$c^{om} = \sum_{k \in K} \left(C_k^{FOM} cp_k^{in} \right) + \sum_{i \in I} W_i \sum_{t \in T} \Delta_t \left[\sum_{p \in P} \left(C_p^{VOM} g_{p,i,t} \right) + \sum_{s \in S} \left(C_s^{VOM} f_{s,i,t}^{+} \right) \right] \tag{3}$$

$$c^{gen} = \sum_{i \in I} W_i \sum_{t \in T} \Delta_t \sum_{p \in H} \left(C_p^{FU} + C_p^{EM} \right) g_{p,i,t} \tag{4}$$

$$c^{flex} = \sum_{i \in I} W_i \sum_{p \in H} \sum_{t \in T} \left(C_p^{SU} u_{p,i,t}^{su} + C_p^{RAMP} ramp_{p,i,t} \right) \tag{5}$$

Equation (6) minimizes the annual GHG emissions related to electricity generation.

$$\min \phi_{GHG} = \sum_{p \in H} \sum_{i \in I} \sum_{t \in T} \left(EF_p W_i \Delta_t g_{p,i,t} \right) \tag{6}$$

Equation (7) minimizes overall social opposition, defined as public resistance to specific generation technologies (e.g., due to perceived catastrophic risks, health concerns, and local impacts). Quantifying social opposition is inherently challenging, as it is an arguably subjective indicator. A common practice in the literature is to operationalize this dimension through technology-level acceptability/opposition ratings expressed on ordinal or Likert scales, typically collected via surveys or expert elicitation [24]. We use expert ratings reported in [28] on a 1–5 scale (from least to highest social opposition) and convert them into a percentage technology-level opposition score (0–100%) via linear rescaling [24]. The system-level social opposition is then computed as the ratio between the generation-weighted sum of technology-level opposition scores and total electricity demand.

$$\min \phi_{SO} = \frac{\sum_{p \in P} \sum_{i \in I} \sum_{t \in T} \left(SO_p W_i \Delta_t g_{p,i,t} \right)}{\sum_{i \in I} \sum_{t \in T} \left(W_i \Delta_t DM_{i,t} \right)} \tag{7}$$

The generation-weighting is adopted to match the system-level scope of the model and to obtain a portfolio-level indicator. However, it should be noted that this approach bears some limitations. The resulting metric does not explicitly capture spatial heterogeneity or site-specific visibility effects, which would typically require spatially resolved siting information. By construction, technologies supplying a larger share of total electricity demand have a proportionally larger influence on the aggregate score. In addition, social acceptability scores may evolve over time and can be context and location dependent. Therefore, the adopted ratings should be interpreted as indicative inputs and are primarily suited to support system-level comparisons of alternative portfolios.

2.3.2. Feasibility Constraints

Equation (8) enforces the power balance at each representative period i and time step t, with electricity supply (generation plus storage discharging) equal to electricity demand plus storage charging.

$$\sum_{p\in P} g_{p,i,t} + \sum_{s\in S} f^{-}_{s,i,t} = DM_{i,t} + \sum_{s\in S} f^{+}_{s,i,t} \quad \forall i,t \tag{8}$$

Equations (9)–(11) define capacity expansion and availability for each technology. Equation (9) ensures that the newly installed capacity for each technology does not exceed the maximum allowed for new investments, while Equation (10) defines the total installed capacity as the sum of existing capacity and newly installed capacity. Unplanned and scheduled outages are captured by derating installed capacity with an availability factor in Equation (11).

$$cp_k^{new} \le CP_k^{MAX} \quad \forall k \tag{9}$$

$$cp_k^{in} = CP_k^{EX} + cp_k^{new} \quad \forall k \tag{10}$$

$$cp_k^{av} \le AF_k cp_k^{in} \quad \forall k \tag{11}$$

Equations (12)–(22) describe the operational constraints of thermal generation technologies under a CUC formulation. Equation (12) relates available capacity to the corresponding number of available units, while Equation (13) limits the number of online units at each representative period and time step. Equation (14) governs the evolution of the commitment state across time steps by accounting for start-up and shut-down events. Equations (15) and (16) enforce minimum and maximum generation limits. Equations (17) and (18) impose ramp-up and ramp-down limits. Equations (19) and (20) compute the effective power ramps between consecutive time steps for ramping-cost evaluation. Equations (21) and (22) enforce minimum up-time and minimum down-time constraints.

$$u_p^{av} \le \frac{cp_p^{av}}{P_p^{MAX}} \quad \forall p \in H \tag{12}$$

$$u_{p,i,t}^{on} \le u_p^{av} \quad \forall p \in H, i, t \tag{13}$$

$$u_{p,i,t+1}^{on} = u_{p,i,t}^{on} + u_{p,i,t}^{su} - u_{p,i,t}^{sd} \quad \forall p \in H, i, t \tag{14}$$

$$g_{p,i,t} \ge P_p^{MIN} u_{p,i,t}^{on} \quad \forall p \in H, i, t \tag{15}$$

$$g_{p,i,t} \le P_p^{MAX} u_{p,i,t}^{on} - \left(P_p^{MAX} - SU_p\right) u_{p,i,t-1}^{su} - \left(P_p^{MAX} - SD_p\right) u_{p,i,t}^{sd} \quad \forall p \in H, i, t \tag{16}$$

$$g_{p,i,t+1} - g_{p,i,t} \le RU_p \Delta_t \left(u_{p,i,t}^{on} - u_{p,i,t}^{sd}\right) - P_p^{MIN} u_{p,i,t}^{sd} + SU_p u_{p,i,t}^{su} \quad \forall p \in H, i, t \tag{17}$$

$$g_{p,i,t} - g_{p,i,t+1} \le RD_p \Delta_t \left(u_{p,i,t}^{on} - u_{p,i,t}^{sd}\right) - P_p^{MIN} u_{p,i,t}^{su} + SD_p u_{p,i,t}^{sd} \quad \forall p \in H, i, t \tag{18}$$

$$ramp_{p,i,t} \ge g_{p,i,t+1} - g_{p,i,t} + P_p^{MIN} u_{p,i,t}^{sd} - SU_p u_{p,i,t}^{su} \quad \forall p \in H, i, t \tag{19}$$

$$ramp_{p,i,t} \ge g_{p,i,t} - g_{p,i,t+1} + P_p^{MIN} u_{p,i,t}^{su} - SD_p u_{p,i,t}^{sd} \quad \forall p \in H, i, t \tag{20}$$

$$u_{p,i,t}^{sd} \le u_{p,i,t}^{on} - \sum_{t'=1}^{MUT_p - 1} u_{p,i,t-t'}^{su} \quad \forall p \in H, i, t \tag{21}$$

$$u_{p,i,t}^{su} \le u_p^{av} - u_{p,i,t}^{on} - \sum_{t'=1}^{MDT_p - 1} u_{p,i,t-t'}^{sd} \quad \forall p \in H, i, t \tag{22}$$

Equation (23) limits variable renewable generation by available capacity and the time-dependent capacity factor, with curtailment accounting for the unused share of available renewable output.

$$g_{p,i,t} + curt_{p,i,t} = CF_{p,i,t} cp_p^{av} \quad \forall p \in R, i, t \tag{23}$$

Equations (24)–(31) define the operational constraints of storage technologies. Charging and discharging power are limited by the available energy capacity and the power-to-energy ratio in Equations (24) and (25). The state of charge (SOC) dynamics are represented using the approach proposed by Poncelet et al. [7], which distinguishes the SOC trajectory in the first and last repetition of each representative period. Specifically, Equation (26) propagates the SOC between consecutive representative periods by accounting for the net energy balance over the W_i repetitions, while Equation (27) updates the SOC across time steps within the first repetition. Equations (28) and (29) reconstruct the SOC of the last repetition consistently with W_i and track its intra-period evolution. Feasibility of the charging and discharging schedule is enforced by the SOC bounds in Equations (30) and (31), which ensure sufficient energy to discharge and adequate headroom to charge at every time step.

$$f_{s,i,t}^{+} \leq PE_s cp_s^{av} \quad \forall s, i, t \tag{24}$$

$$f_{s,i,t}^{-} \leq PE_s cp_s^{av} \quad \forall s, i, t \tag{25}$$

$$soc_{s,i+1,t=1}^{fr} = soc_{s,i,t=1}^{fr} + W_i \sum_{t \in T} \Delta_t \left(\sqrt{RT_s} f_{s,i,t}^{+} - \frac{f_{s,i,t}^{-}}{\sqrt{RT_s}} \right) \quad \forall s, i \tag{26}$$

$$soc_{s,i,t+1}^{fr} = soc_{s,i,t}^{fr} + \Delta_t \left(\sqrt{RT_s} f_{s,i,t}^{+} - \frac{f_{s,i,t}^{-}}{\sqrt{RT_s}} \right) \quad \forall s, i, t : t \neq |T| \tag{27}$$

$$soc_{s,i,t=1}^{lr} = soc_{s,i,t=1}^{fr} + (W_i - 1) \sum_{t \in T} \Delta_t \left(\sqrt{RT_s} f_{s,i,t}^{+} - \frac{f_{s,i,t}^{-}}{\sqrt{RT_s}} \right) \quad \forall s, i \tag{28}$$

$$soc_{s,i,t+1}^{lr} = soc_{s,i,t}^{lr} + \Delta_t \left(\sqrt{RT_s} f_{s,i,t}^{+} - \frac{f_{s,i,t}^{-}}{\sqrt{RT_s}} \right) \quad \forall s, i, t : t \neq |T| \tag{29}$$

$$\Delta_t \frac{f_{s,i,t}^{-}}{\sqrt{RT_s}} \leq soc_{s,i,t}^{fr} \leq cp_s^{av} - \Delta_t \sqrt{RT_s} f_{s,i,t}^{+} \quad \forall s, i, t \tag{30}$$

$$\Delta_t \frac{f_{s,i,t}^{-}}{\sqrt{RT_s}} \leq soc_{s,i,t}^{lr} \leq cp_s^{av} - \Delta_t \sqrt{RT_s} f_{s,i,t}^{+} \quad \forall s, i, t \tag{31}$$

2.4. Experimental Design

This section describes the experimental design adopted to evaluate the proposed model. Section 2.4.1 presents the Italian case study to which the proposed model is applied, Section 2.4.2 outlines the analysis performed, and Section 2.4.3 reports the experimental setup used.

2.4.1. Italian Case Study

An application of the proposed model to the Italian electricity system is carried out to test its practical applicability in a real-world context. Specifically, the case study explores the synergies and trade-offs among cost, GHG emissions, and social opposition for the 2040 planning horizon, with 2040 treated as the target year.

The analysis adopts a brownfield setting, with the 2024 capacity portfolio used as the initial system configuration and additional capacity allowed through new investments. To retain operational realism while keeping the problem computationally tractable, the target year is represented through 8 weighted representative days with hourly resolution,

selected using the optimization-based method proposed by Poncelet et al. [8]. In that study, the authors benchmark their optimization-based selection against alternative approaches across different numbers of representative days. They show that accuracy improvements in capturing temporal variability (e.g., duration-curve metrics) exhibit diminishing returns as the number of representative days increases, while computational effort grows nonlinearly with the number of time steps in planning models. In particular, for their optimization-based selection, they report sub-percent average approximation errors on duration curves already with 8 representative days. This trade-off supports the use of a limited number of representative days in computationally demanding planning studies. In addition, according to the CUC formulation, similar thermal generation technologies (e.g., natural gas generators) within Italy are aggregated into clusters.

According to Terna [29], the Italian transmission system operator (TSO), Italy's installed generation capacity in 2024 includes about 23.6 GW hydropower, 13 GW onshore wind, 0.8 GW geothermal, 37 GW solar PV, 4 GW bioenergy, and 62.5 GW fossil-fuel capacity (predominantly natural gas, about 55 GW). Electricity storage is dominated by utility-scale pumped hydro storage (PHS), with an energy capacity of about 53 GWh, while battery energy storage systems (BESS) account for approximately 6.8 GWh.

The input data, used to feed the model, are partially derived from previous works of the authors [30,31]. An overview of the main input data categories and their sources is provided in Table 2.

Table 2. Data sources used in the application of the proposed three-objective optimization model to the Italian case study.

Data	Sources and References
Existing capacity	Terna [29], GEM [32], ENTSO-E [33]
Capacity for new investment	Terna [34]
Renewable capacity factors	Terna [29], EMHIRES [35]
Electricity demand	Terna [29,34]
Investment, FOM, VOM costs	European Commission [36], Terna [37]
Fuel cost and carbon tax	Terna [34]
Cycling features of thermal generators	Poncelet [7]
Cycling features of storage systems	Poncelet [7]
Emission factors	UNECE [38]
Social opposition	Grafakos [28], Shidhani [24]

Starting from the 2024 baseline, the capacity mix is allowed to evolve through investments in additional capacity. The evolution trajectory for this scenario is consistent with the Italian planning and policy outlook reported in [34]. The changes to the 2024 baseline are the following:

- In line with the national coal phase-out schedule, coal-fired power plants are assumed to be fully decommissioned.
- New generation and storage investments are allowed in natural gas, solar PV, onshore wind, offshore wind, small nuclear reactors, PHS, and BESS.
- VRE availability is highly sensitive to the selected weather year. Following Lombardi et al. [39], we adopt 2016 as the reference weather year for Italy. In that study, 2016 is identified as the most-typical reference weather year for Italy by screening historical weather years (1981–2016) and assessing how each year affects the minimum-cost system configuration.

2.4.2. Analysis Conducted

The analysis is structured to characterize the trade-offs among the three objectives and to interpret their implications in terms of optimal capacity expansion and system operation.

First, the anchor points (APs) are computed by optimizing each objective individually, i.e., the cost-optimal, emissions-optimal, and social-optimal solutions. These extreme solutions provide interpretable benchmarks and define the boundaries of the attainable objective space. Subsequently, a set of Pareto-efficient (non-dominated) solutions is generated to represent the attainable trade-offs among objectives, i.e., solutions for which improving one objective necessarily deteriorates at least one of the others.

To support the identification of a representative compromise configuration, a best balance solution is selected by minimizing the Euclidean distance to the utopia point (UP). The UP is defined as the vector collecting the best value of each objective across the anchor solutions. Since the UP is typically unattainable in the feasible set due to conflicting objectives, the minimum-distance criterion provides a systematic way to select a Pareto-efficient compromise solution that is close to the ideal performance across all objectives. To ensure comparability across objectives with different units and scales, the distance is evaluated in a normalized objective space.

Given a Pareto-efficient solution, the value of each objective is normalized as in Equation (32), where Φ_n^{best} and Φ_n^{worst} denote the best and worst values of objective n across the APs.

$$\widetilde{\Phi}_n(x) = \frac{\Phi_n(x) - \Phi_n^{best}}{\Phi_n^{worst} - \Phi_n^{best}} \quad \forall n \in N \tag{32}$$

With the normalization in Equation (32), the normalized UP corresponds to the origin (i.e., the zero vector). Therefore, the Euclidean distance to the UP in the normalized objective space, $d(x)$, can be computed as in Equation (33). The best balance solution is selected as the Pareto-efficient solution that minimizes $d(x)$.

$$d(x) = \sqrt{\sum_{n \in N} \widetilde{\Phi}_n(x)^2} \tag{33}$$

The selected best balance solution is then analyzed alongside the APs in terms of (i) the optimal capacity-expansion decisions (technology selection and sizing) and (ii) the corresponding optimal operational schedules (generation mix, renewable curtailment, and storage charging/discharging).

2.4.3. Experimental Setup

The model is implemented in AMPL (AMPL Optimization, Inc., Mountain View, CA, USA) and solved with Gurobi Optimizer v11.0.3 (Gurobi Optimization, LLC, Beaverton, OR, USA). All computations were carried out on a workstation equipped with an AMD Ryzen™ 9 7845HX CPU @ 3.00 GHz and 16 GB of RAM.

For the Italian case study, the CUC formulation is adopted in its relaxed version, where commitment variables are defined as continuous cluster-level variables. Under this assumption, the overall problem reduces to an LP formulation. As discussed in Section 2.3, the proposed formulation also allows solving the CUC component as a MILP by enforcing integer commitment variables. Relaxing integrality may smooth discrete commitment transitions at the cluster level and may affect the valuation of start-up and ramping-related operating costs, with implications for flexibility assessment. As highlighted in the literature, using continuous rather than integer commitment variables can reduce the computational burden while having a limited impact on accuracy [7]. In particular, benchmarking evidence discussed by Poncelet et al. [7] reports sub-percent deviations in total

system cost between integer commitment and continuous commitment variants, together with order-of-magnitude reductions in computation time. They also report that the errors introduced by using a formulation that includes all UC constraints but uses continuous instead of integer commitment variables are significantly lower than the impact of the choice of cycling capabilities of thermal generators.

The Pareto frontier of the three-objective problem is constructed using the NNC method. The resulting set represents the non-dominated (Pareto-efficient) solutions in the objective space. In this study, each Pareto point is characterized by the value of the total annual system cost, Equation (1), annual GHG emissions, Equation (6), and social opposition, Equation (7).

For the Italian case study, the resulting optimization problem comprises 39,805 variables (all continuous) and 41,174 constraints.

3. Results

The results obtained from the model application to the Italian case study are presented in the following sections.

3.1. Pareto Frontier

Figure 2 shows the set of non-dominated (Pareto-efficient) solutions obtained with the NNC method in the three-dimensional objective space (cost, GHG emissions, and social opposition). Each point represents a feasible power system configuration. The three APs, obtained by optimizing each objective separately, are highlighted in gray. AP1 corresponds to the cost-optimal solution, AP2 to the emissions-optimal solution, and AP3 to the social-optimal solution. The best balance (BB) solution, selected by minimizing the Euclidean distance to the UP, is highlighted in red. The generation of the Pareto frontier required approximately 2 h, with an average computational time of about 10 s per point.

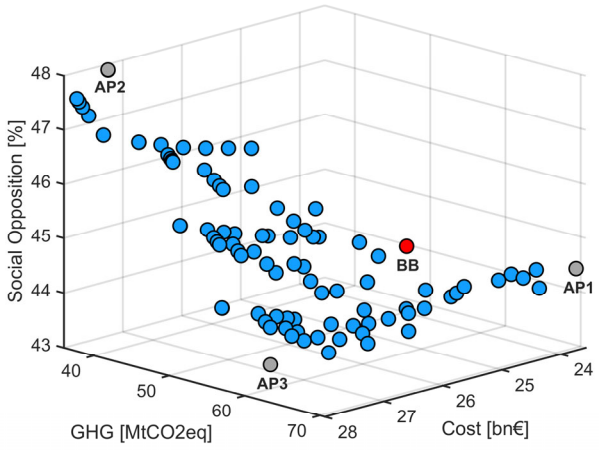

Figure 2. Pareto-efficient solutions for the Italian case study in the three-dimensional objective space defined by cost, GHG emissions, and social opposition.

Table 3 reports the objective values and derived indicators for the three APs and for the BB solution.

Table 3. Objective values and derived indicators for the anchor points and the best balance solution.

Category	Unit	AP1	AP2	AP3	BB
total cost	[bn€]	23.6	27.3	28.0	24.8
GHG emissions	[$MtCO_2eq$]	69.8	36.0	63.0	56.5

social opposition	[%]	44.4	47.9	43.6	44.7
avg cost per MWh	[€/MWh]	60.4	69.5	72.0	63.4
carbon intensity	[gCO_2eq/kWh]	178.6	91.6	161.2	144.4

AP1 (cost-optimal) yields the lowest total cost (23.6 bn€) with 69.8 $MtCO_2eq$ and 44.4% social opposition. AP2 (emissions-optimal) achieves the minimum GHG emissions (36.0 $MtCO_2eq$) with 27.3 bn€ and 47.9% social opposition. AP3 (social-optimal) attains the lowest social opposition (43.6%) with 28.0 bn€ and 63.0 $MtCO_2eq$. The BB solution lies between AP1 and AP2 for cost (24.8 bn€) and between AP2 and AP3 for GHG emissions (56.5 $MtCO_2eq$), while keeping social opposition close to AP1 (44.7%).

In terms of derived indicators, the average electricity cost ranges from 60.4 €/MWh (AP1) to 72.0 €/MWh (AP3), with BB at 63.4 €/MWh. Carbon intensity ranges from 91.6 gCO_2eq/kWh (AP2) to 178.6 gCO_2eq/kWh (AP1), with BB at 144.4 gCO_2eq/kWh.

3.2. Capacity Expansion Planning

Figure 3 reports the new capacity additions by technology for the APs and the BB solution, disaggregated into generation (Figure 3a) and storage (Figure 3b).

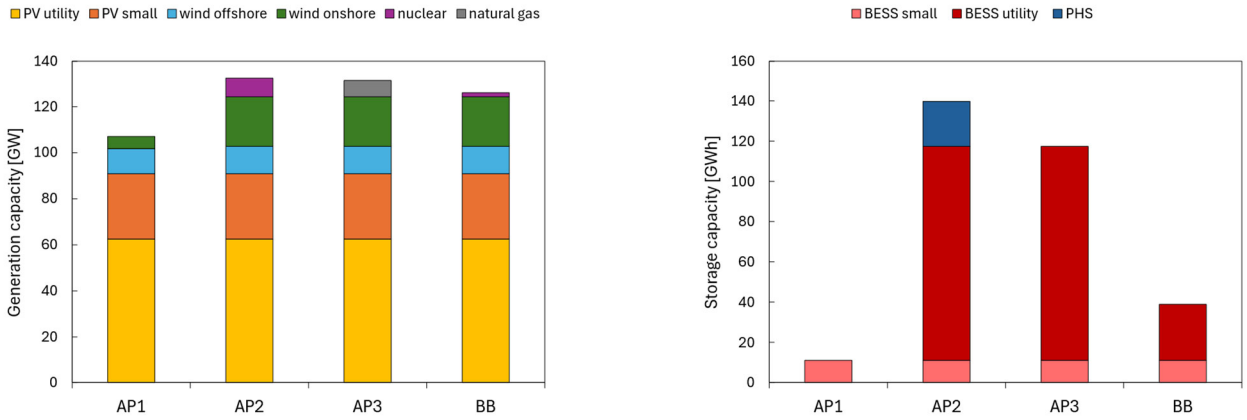

(**a**) (**b**)

Figure 3. New capacity additions by technology for the anchor points and the best balance solution: (**a**) generation capacity; (**b**) storage capacity.

Across all configurations, solar PV provides the largest share of new generation capacity, and both utility-scale and small-scale PV additions are identical in the four solutions. Investments in new wind capacity are observed in all configurations, including both onshore and offshore components. Offshore additions are identical across all cases, whereas onshore additions differ only in AP1, where the new capacity is lower than in the other configurations. Concerning dispatchable capacity, AP1 exhibits no additions, nuclear investments are introduced in AP2 and remain marginal in BB, whereas natural-gas investments occur only in AP3.

On the storage side, small-scale BESS additions are identical across all solutions. In AP1, storage expansion is limited to small-scale BESS additions. In contrast, AP2 and AP3 deploy substantial additional storage dominated by utility-scale BESS, with AP2 also featuring new PHS capacity. The BB solution shows a moderate storage expansion, consisting of both utility-scale and small-scale BESS.

3.3. Operational Schedules

Figure 4 shows the generation mix (Figure 4a) and renewable curtailment (Figure 4b) for the APs and the BB solution.

AP1 shows the lowest renewable share (56%), with natural gas supplying the remaining 44% of total generation. The other solutions feature similar renewable shares (around 60%), while nuclear generation differs across them, accounting for 15% in AP2, being absent in AP3, and reaching 4% in BB. Accordingly, the share of natural gas decreases to 23% in AP2, while it remains higher in AP3 (38%) and BB (36%). Renewable curtailment varies across solutions, ranging from about 0.5 TWh in AP2 to about 8 TWh in AP1, with intermediate values of 1.4 TWh in AP3 and 6.4 TWh in the BB solution.

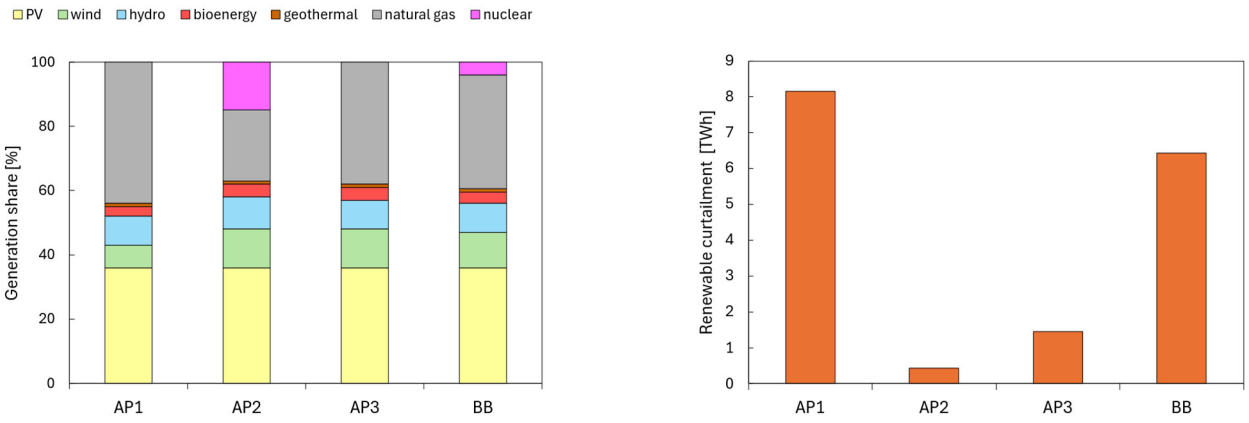

(**a**) (**b**)

Figure 4. Generation mix and renewable curtailment for the anchor points and the best balance solution: (**a**) generation shares by technology; (**b**) curtailed renewable energy.

Figure 5 shows the average hourly profiles of aggregated storage operation and renewable curtailment for AP1 (Figure 5a), AP2 (Figure 5b), AP3 (Figure 5c), and the BB solution (Figure 5d), with positive and negative values denoting charging and discharging, respectively.

Figure 5 highlights a recurring diurnal pattern in storage operation across all cases, with charging concentrated in the central hours of the day and discharging mainly occurring during night-time and early-morning hours. The amplitude of storage operation differs across solutions. Charging and discharging volumes are highest in AP2 and lowest in AP1, with AP3 and the BB solution showing intermediate values. In all cases, renewable curtailment is concentrated around mid-day, with lower levels in AP2 and AP3 and higher levels in AP1 and the BB solution.

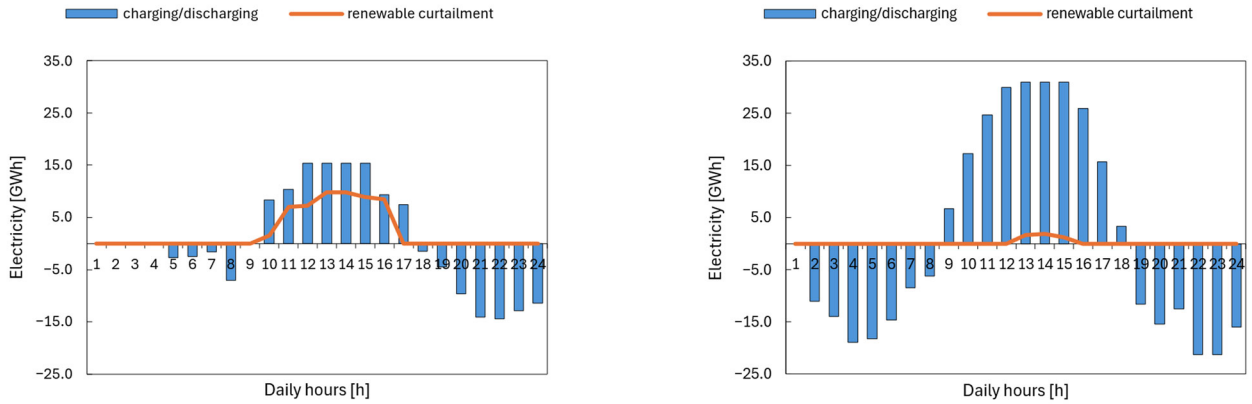

(**a**) (**b**)

https://doi.org/10.3390/app16062946

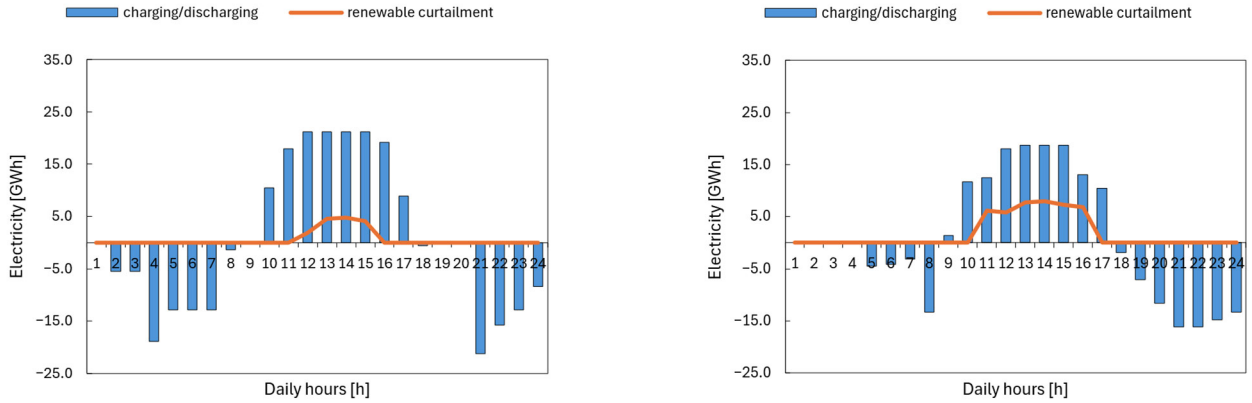

(**c**) (**d**)

Figure 5. Average daily hourly profiles of storage operation and renewable curtailment: (**a**) AP1 (cost-optimal); (**b**) AP2 (emissions-optimal); (**c**) AP3 (social-optimal); (**d**) BB (best balance).

4. Discussion

This section discusses the main insights from the Italian case study by interpreting the three-objective trade-off surface (Section 4.1) and its implications for expansion and operation decisions (Section 4.2). It then summarizes the methodological and managerial insights of the proposed modeling approach (Section 4.3).

4.1. Trade-Off Analysis

The Pareto set of efficient solutions confirms that the three objectives are conflicting, and decision support benefits from an explicit representation of the attainable trade-off surface. The cost-optimal solution (AP1) minimizes expenditure but results in comparatively high emissions, reflecting the continued role of natural-gas generation and limited additional flexibility. Conversely, the emissions-optimal solution (AP2) achieves the lowest carbon footprint but requires a marked cost increase, consistent with a system that relies more strongly on low-carbon firm generation and greater flexibility provision. The social-optimal solution (AP3) attains the lowest social opposition at a further cost premium and with emissions remaining substantially higher than AP2. This highlights that resistance to specific technologies such as nuclear does not necessarily align with deep decarbonization pathways. The best balance (BB) solution provides a compromise among the objectives. Compared to AP1, it delivers a sizable emissions reduction (≈20%) for a limited cost increase (≈5%) and a marginal increase in social opposition (≈0.7%).

A further observation is that the attainable range of social opposition is comparatively narrow relative to the ranges of costs and emissions. This behavior is consistent with the adopted metric, defined as the ratio between the generation-weighted sum of technology-level opposition scores and total electricity demand. Under this definition, the social opposition score is dominated by technologies contributing most to annual dispatch. When dispatch remains concentrated on technologies with similar opposition scores and when their shares vary moderately across efficient solutions, the system-level average changes only slightly. In this setting, the social objective is therefore most informative through portfolio effects (e.g., the deployment of contested firm low-carbon options such as nuclear), rather than through large movements of the aggregated index.

From a policy perspective, the proposed indicator is intended to support system-level comparisons of alternative generation portfolios and to highlight how contested options affect compromise solutions in the three-objective space. It should not be interpreted as a siting or permitting metric, since local acceptance is shaped by spatial heterogeneity and

visibility-related factors that are not represented in the present system-level formulation. Accordingly, complementary spatially explicit analyses and participatory assessments are required when the focus is on location-specific deployment decisions.

4.2. Capacity Expansion Implications

Across the Pareto set, VRE deployment emerges as a consistent expansion signal, confirming its central role in the Italian 2040 transition. Differences among efficient solutions are driven mainly by the amount and composition of flexibility investments and the role of dispatchable and firm low-carbon technologies. Moving from cost-oriented to emissions-oriented solutions systematically increases the need for flexibility and reduces reliance on unabated thermal dispatch, reflecting the increasing value of flexibility at high VRE penetration. Conversely, minimizing social opposition can constrain the adoption of specific firm low-carbon options such as nuclear.

Operational outcomes provide a coherent interpretation of these expansion patterns. Storage follows a consistent diurnal behavior, with charging aligned with periods of high VRE availability and discharging shifted toward hours with higher residual demand. Differences among solutions are reflected in the intensity of storage cycling and in curtailment levels. Emissions-oriented solutions typically reduce curtailment through stronger flexibility provision and a lower reliance on thermal balancing, whereas cost-oriented solutions accept higher curtailment and rely more on dispatchable generation to maintain feasibility at lower total cost. Overall, the case study shows that flexibility investments and operational constraints jointly shape the achievable trade-offs and the role of storage and dispatchable resources.

In the cost-optimal solution (AP1), investments in capital-intensive options such as nuclear and large-scale storage are not selected, and the system relies on the existing dispatchable capacity while accepting higher curtailment and emissions. In the emissions-optimal solution (AP2), nuclear investments emerge as a firm low-carbon option, and the system places a higher value on additional storage flexibility to reduce natural-gas generation and curtailment. In this context, PHS is selected as a long-duration flexibility option that complements BESS. In the social-optimal solution (AP3), minimizing social opposition discourages nuclear and favors additional natural-gas capacity as a source of firm flexibility. Consistently, no new PHS capacity is installed, and investments in additional storage capacity are concentrated in BESS. This outcome can be interpreted as reflecting both the reduced marginal value of long-duration storage when additional firm flexibility is provided by natural gas and the lower round-trip efficiency of PHS compared to BESS.

It should be noted that the Italian system is represented as a single node and therefore does not capture transmission constraints, network congestion, or the spatial heterogeneity of renewable potentials. This copperplate assumption may affect both renewable integration and flexibility valuation, for instance by yielding optimistic system-wide balancing and curtailment estimates when VRE production is geographically concentrated, and by shifting the relative role of flexibility options (e.g., storage versus transmission reinforcement or local dispatchable capacity) compared with a spatially resolved formulation. Accordingly, the results should be interpreted as system-level insights under the adopted aggregation, while a multi-node extension with explicit transmission constraints is expected to refine the quantification of flexibility needs and VRE integration limits.

4.3. Methodological and Managerial Insights

From a methodological standpoint, the proposed modeling approach shows that three-objective planning can remain tractable while retaining a high level of temporal and operational detail. Weighted representative periods compress the annual horizon while preserving intra-period dynamics that are necessary to represent VRE variability and

flexibility needs. In addition, the CUC retains key commitment decisions and operating constraints with a reduced combinatorial burden relative to BUC.

From a managerial perspective, the Pareto frontier supports a transparent comparison of efficient alternatives and helps identify compromise regions where meaningful emissions reductions are achievable at limited cost premiums with only marginal changes in social opposition, avoiding over-reliance on single-objective optima. Moreover, incorporating a high level of temporal and operational detail can improve the interpretability of expansion plans by linking capacity choices to feasible dispatch patterns under high VRE penetration.

5. Conclusions and Future Research

This paper presents a three-objective optimization model for sustainable power system design that simultaneously accounts for costs, GHG emissions, and social opposition. The model adopts weighted representative periods with intra-period time steps to preserve temporal variability while maintaining tractability, and it integrates detailed operational constraints through a CUC formulation, which preserves key commitment decisions while reducing the computational burden compared with BUC. The resulting Pareto-efficient solutions, generated using the NNC method, provide a transparent basis for decision-making, since they render trade-offs explicit rather than embedding preferences a priori.

The Italian case study illustrates that the three sustainability objectives are conflicting, and that the Pareto set supports the identification of balanced compromises. In particular, the best balance solution identified shows that non-trivial GHG emissions reductions can be achieved with a relatively modest increase in system costs, while maintaining a limited change in social opposition. Conversely, the anchor solutions highlight how prioritizing a single sustainability dimension can imply markedly different expansion strategies and operational patterns, confirming the value of multi-objective formulations for transparent decision-making. Results also emphasize the central role of flexibility investments in reducing curtailment and enabling higher renewable shares, and they show how social preferences can reshape decarbonization pathways by discouraging specific technologies such as nuclear.

The proposed modeling approach provides a tractable and operationally informed basis to support sustainable power system design. However, it presents some limitations that suggest clear directions for future work. The quantitative outcomes of the Italian case study are conditional to key input assumptions (e.g., social opposition coefficients, carbon pricing, 2040 cost projections, weather year selection, and representative period selection). The analysis can be further strengthened in future work through scenario-based studies and targeted sensitivity assessments for these inputs. The current formulation relies on a single-node representation and therefore cannot capture spatially differentiated renewable potentials, network congestion, and the role of transmission expansion. Extending the model to a multi-node setting with explicit transmission constraints and reinforcement options could improve the realism of balancing strategies and flexibility valuation under high VRE penetration. The model represents a target year rather than a multi-year transition. A multi-year formulation could enable a consistent treatment of technology lead times and decommissioning trajectories, investment phasing, and evolving operational conditions across the planning horizon. Furthermore, incorporating uncertainty in demand, technology costs, fuel prices, and renewable availability could improve the robustness of the derived trade-offs and reduce the risk of results that are overly sensitive to input assumptions.

https://doi.org/10.3390/app16062946

Author Contributions: Conceptualization, C.C.; methodology, C.C.; software, C.C.; validation, C.C.; formal analysis, C.C.; investigation, C.C.; resources, M.B. and M.G.; data curation, C.C.; writing—original draft preparation, C.C.; writing—review and editing, C.C., M.R. and F.G.G.; visualization, C.C. and M.R.; supervision, F.G.G., M.B. and M.G.; project administration, M.B. and M.G.; funding acquisition, M.B. and M.G. All authors have read and agreed to the published version of the manuscript.

Funding: This research received no external funding.

Institutional Review Board Statement: Not applicable.

Informed Consent Statement: Not applicable.

Data Availability pStatement: Data will be made available by the authors upon request.

Conflicts of Interest: The authors declare no conflicts of interest.

Abbreviations

The following abbreviations are used in this manuscript:

AHP	Analytic hierarchy process
AP	Anchor point
BESS	Battery energy storage systems
BUC	Binary unit commitment
CUC	Clustered unit commitment
EC	ε-constraint
GHG	Greenhouse gas
LP	Linear programming
MILP	Mixed-integer linear programming
MOEA	Multi-objective evolutionary algorithms
NNC	Normalized normal constraint
NPV	Net present value
PHS	Pumped hydro storage
PV	Photovoltaic
RPM	Reference point method
SOC	State of charge
TSO	Transmission system operator
UC	Unit commitment
UP	Utopia point
VRE	Variable renewable energy
WS	Weighted sum

References

1. Akpahou, R.; Mensah, L.D.; Quansah, D.A.; Kemausuor, F. Energy Planning and Modeling Tools for Sustainable Development: A Systematic Literature Review. *Energy Rep.* **2024**, *11*, 830–845. https://doi.org/10.1016/j.egyr.2023.11.043.
2. Das, S.; Dutta, R.; De, S.; De, S. Review of Multi-Criteria Decision-Making for Sustainable Decentralized Hybrid Energy Systems. *Renew. Sustain. Energy Rev.* **2024**, *202*, 114676. https://doi.org/10.1016/j.rser.2024.114676.
3. Chen, W.; Ren, H.; Zhou, W. Review of Multi-Objective Optimization in Long-Term Energy System Models. *Glob. Energy Interconnect.* **2023**, *6*, 645–660. https://doi.org/10.1016/j.gloei.2023.10.010.
4. Prina, M.G.; Manzolini, G.; Moser, D.; Nastasi, B.; Sparber, W. Classification and Challenges of Bottom-up Energy System Models—A Review. *Renew. Sustain. Energy Rev.* **2020**, *129*, 109917. https://doi.org/10.1016/j.rser.2020.109917.
5. Khan, S.A.; Tao, Z.; Agyekum, E.B.; Fahad, S.; Tahir, M.; Salman, M. Sustainable rural electrification: Energy-economic feasibility analysis of autonomous hydrogen-based hybrid energy system. *Int. J. Hydrogen Energy* **2025**, *141*, 460–473. https://doi.org/10.1016/j.ijhydene.2024.09.063.
6. Poncelet, K.; Delarue, E.; Six, D.; Duerinck, J.; D'haeseleer, W. Impact of the Level of Temporal and Operational Detail in Energy-System Planning Models. *Appl. Energy* **2016**, *162*, 631–643. https://doi.org/10.1016/j.apenergy.2015.10.100.

7. Poncelet, K.; Delarue, E.; D'haeseleer, W. Unit Commitment Constraints in Long-Term Planning Models: Relevance, Pitfalls and the Role of Assumptions on Flexibility. *Appl. Energy* **2020**, *258*, 113843. https://doi.org/10.1016/j.apenergy.2019.113843.
8. Poncelet, K.; Hoschle, H.; Delarue, E.; Virag, A.; Drhaeseleer, W. Selecting Representative Days for Capturing the Implications of Integrating Intermittent Renewables in Generation Expansion Planning Problems. *IEEE Trans. Power Syst.* **2017**, *32*, 1936–1948. https://doi.org/10.1109/tpwrs.2016.2596803.
9. Meus, J.; Poncelet, K.; Delarue, E. Applicability of a Clustered Unit Commitment Model in Power System Modeling. *IEEE Trans. Power Syst.* **2018**, *33*, 2195–2204. https://doi.org/10.1109/tpwrs.2017.2736441.
10. Purwanto, W.W.; Pratama, Y.W.; Nugroho, Y.S.; Warjito; Hertono, G.F.; Hartono, D.; Deendarlianto; Tezuka, T. Multi-Objective Optimization Model for Sustainable Indonesian Electricity System: Analysis of Economic, Environment, and Adequacy of Energy Sources. *Renew. Energy* **2015**, *81*, 308–318. https://doi.org/10.1016/j.renene.2015.03.046.
11. Gbadamosi, S.L.; Nwulu, N.I. A Multi-Period Composite Generation and Transmission Expansion Planning Model Incorporating Renewable Energy Sources and Demand Response. *Sustain. Energy Technol. Assess.* **2020**, *39*, 100726. https://doi.org/10.1016/j.seta.2020.100726.
12. Pratama, Y.W.; Purwanto, W.W.; Tezuka, T.; McLellan, B.C.; Hartono, D.; Hidayatno, A.; Daud, Y. Multi-Objective Optimization of a Multiregional Electricity System in an Archipelagic State: The Role of Renewable Energy in Energy System Sustainability. *Renew. Sustain. Energy Rev.* **2017**, *77*, 423–439. https://doi.org/10.1016/j.rser.2017.04.021.
13. Groissböck, M.; Pickl, M.J. An Analysis of the Power Market in Saudi Arabia: Retrospective Cost and Environmental Optimization. *Appl. Energy* **2016**, *165*, 548–558. https://doi.org/10.1016/j.apenergy.2015.12.086.
14. Finke, J.; Bertsch, V. Implementing a Highly Adaptable Method for the Multi-Objective Optimisation of Energy Systems. *Appl. Energy* **2023**, *332*, 120521. https://doi.org/10.1016/j.apenergy.2022.120521.
15. Louis, J.N.; Allard, S.; Kotrotsou, F.; Debusschere, V. A Multi-Objective Approach to the Prospective Development of the European Power System by 2050. *Energy* **2020**, *191*, 116539. https://doi.org/10.1016/j.energy.2019.116539.
16. Prina, M.G.; Lionetti, M.; Manzolini, G.; Sparber, W.; Moser, D. Transition Pathways Optimization Methodology through EnergyPLAN Software for Long-Term Energy Planning. *Appl. Energy* **2019**, *235*, 356–368. https://doi.org/10.1016/j.apenergy.2018.10.099.
17. Prina, M.G.; Casalicchio, V.; Kaldemeyer, C.; Manzolini, G.; Moser, D.; Wanitschke, A.; Sparber, W. Multi-Objective Investment Optimization for Energy System Models in High Temporal and Spatial Resolution. *Appl. Energy* **2020**, *264*, 114728. https://doi.org/10.1016/j.apenergy.2020.114728.
18. Viesi, D.; Crema, L.; Mahbub, M.S.; Verones, S.; Brunelli, R.; Baggio, P.; Fauri, M.; Prada, A.; Bello, A.; Nodari, B.; et al. Integrated and Dynamic Energy Modelling of a Regional System: A Cost-Optimized Approach in the Deep Decarbonisation of the Province of Trento (Italy). *Energy* **2020**, *209*, 118378. https://doi.org/10.1016/j.energy.2020.118378.
19. Prina, M.G.; Fanali, L.; Manzolini, G.; Moser, D.; Sparber, W. Incorporating Combined Cycle Gas Turbine Flexibility Constraints and Additional Costs into the EPLANopt Model: The Italian Case Study. *Energy* **2018**, *160*, 33–43. https://doi.org/10.1016/j.energy.2018.07.007.
20. Cafarella, C.; Gamberi, M.; Bortolini, M.; Galizia, F.G.; Delarue, E. A Multiobjective Optimization Model to Balance Costs and Land Use in Power System Expansion Planning. In *Sustainable Design and Manufacturing 2024*; Jolly, M., Scholz, S.G., Howlett, R.J., Setchi, R., Eds.; Smart Innovation, Systems and Technologies; Springer: Singapore, 2025; Volume 112, pp. 339–351. https://doi.org/10.1007/978-981-96-4459-9_31.
21. Peng, Q.; Liu, W.; Shi, Y.; Dai, Y.; Yu, K.; Graham, B. Multi-Objective Electricity Generation Expansion Planning towards Renewable Energy Policy Objectives under Uncertainties. *Renew. Sustain. Energy Rev.* **2024**, *197*, 114406. https://doi.org/10.1016/j.rser.2024.114406.
22. Prebeg, P.; Gasparovic, G.; Krajacic, G.; Duic, N. Long-Term Energy Planning of Croatian Power System Using Multi-Objective Optimization with Focus on Renewable Energy and Integration of Electric Vehicles. *Appl. Energy* **2016**, *184*, 1493–1507. https://doi.org/10.1016/j.apenergy.2016.03.086.
23. Parkinson, S.C.; Makowski, M.; Krey, V.; Sedraoui, K.; Almasoud, A.H.; Djilali, N. A Multi-Criteria Model Analysis Framework for Assessing Integrated Water-Energy System Transformation Pathways. *Appl. Energy* **2018**, *210*, 477–486. https://doi.org/10.1016/j.apenergy.2016.12.142.
24. Al Shidhani, T.; Ioannou, A.; Falcone, G. Multi-Objective Optimisation for Power System Planning Integrating Sustainability Indicators. *Energies* **2020**, *13*, 2199. https://doi.org/10.3390/en13092199.

25. Trotter, P.A.; Cooper, N.J.; Wilson, P.R. A Multi-Criteria, Long-Term Energy Planning Optimisation Model with Integrated on-Grid and off-Grid Electrification—The Case of Uganda. *Appl. Energy* **2019**, *243*, 288–312. https://doi.org/10.1016/j.apenergy.2019.03.178.
26. Atabaki, M.S.; Aryanpur, V. Multi-Objective Optimization for Sustainable Development of the Power Sector: An Economic, Environmental, and Social Analysis of Iran. *Energy* **2018**, *161*, 493–507. https://doi.org/10.1016/j.energy.2018.07.149.
27. Gonzato, S.; Bruninx, K.; Delarue, E. Long Term Storage in Generation Expansion Planning Models with a Reduced Temporal Scope. *Appl. Energy* **2021**, *298*, 117168. https://doi.org/10.1016/j.apenergy.2021.117168.
28. Grafakos, S.; Flamos, A. Assessing Low-Carbon Energy Technologies against Sustainability and Resilience Criteria: Results of a European Experts Survey. *Int. J. Sustain. Energy* **2017**, *36*, 502–516. https://doi.org/10.1080/14786451.2015.1047371.
29. Terna. Portale Dati. Available online: https://dati.terna.it/en/ (accessed on 19 December 2025).
30. Bortolini, M.; Cafarella, C.; Galizia, F.G.; Gamberi, M. Energy System Optimization Modelling and Electrical Grid Management: The Case of Italy. In *Production Processes and Product Evolution in the Age of Disruption*; Galizia, F.G., Bortolini, M., Eds.; Lecture Notes in Mechanical Engineering; Springer: Cham, Switzerland, 2023; pp. 495–505. https://doi.org/10.1007/978-3-031-34821-1_54.
31. Cafarella, C.; Bortolini, M.; Gabellini, M.; Galizia, F.G.; Ventura, V. Energy Network Optimization Model for Supporting Generation Expansion Planning and Grid Design. In *Sustainable Design and Manufacturing 2023*; Scholz, S.G., Howlett, R.J., Setchi, R., Eds.; Smart Innovation, Systems and Technologies; Springer: Singapore, 2024; Volume 377, pp. 239–251. https://doi.org/10.1007/978-981-99-8159-5_21.
32. GEM. Global Energy Monitor. Available online: https://globalenergymonitor.org/projects/ (accessed on 19 December 2025).
33. ENTSO-E. European Network of Transmission System Operators for Electricity. Available online: https://www.entsoe.eu/ (accessed on 19 December 2025).
34. Terna. Documento Di Descrizione Degli Scenari 2024. Available online: https://download.terna.it/terna/Documento_Descrizione_Scenari_2024_8dce2430d44d101.pdf (accessed on 19 December 2025).
35. EMHIRES. European Meteorological Derived High Resolution RES Generation Time Series for Present and Future Scenarios. Available online: https://data.jrc.ec.europa.eu/collection/id-0055#datasets (accessed on 19 December 2025).
36. European Commission. *Asset Study on Technology Pathways in Decarbonisation Scenarios*; Publications Office of the European Union: Luxembourg, 2020. https://doi.org/10.2833/994817.
37. Terna. Study on Reference Technologies for Electricity Storage. Available online: https://download.terna.it/terna/Study_on_electricity_storage_reference_technologies_8db99b53d98c32b.pdf (accessed on 19 December 2025).
38. UNECE. Life Cycle Assessment of Electricity Generation Options. Available online: https://unece.org/sed/documents/2021/10/reports/life-cycle-assessment-electricity-generation-options (accessed on 27 January 2026).
39. Lombardi, F.; Pickering, B.; Colombo, E.; Pfenninger, S. Policy Decision Support for Renewables Deployment through Spatially Explicit Practically Optimal Alternatives. *Joule* **2020**, *4*, 2185–2207. https://doi.org/10.1016/J.JOULE.2020.08.002.